

Predicted Signs of One-Bond Spin–Spin Coupling Constants (${}^1J_{\text{H-Y}}$) across X–H–Y Hydrogen Bonds for Complexes with Y = ${}^{15}\text{N}$, ${}^{17}\text{O}$, and ${}^{19}\text{F}$

Janet E. Del Bene^{*,†} and José Elguero[‡]

Department of Chemistry, Youngstown State University, Youngstown, Ohio 44555, and Instituto de Química Médica, CSIC, Juan de la Cierva, 3, E-28006 Madrid, Spain

Received: August 11, 2004; In Final Form: October 1, 2004

Ab initio equation-of-motion coupled cluster (EOM-CCSD) calculations have been performed on a set of 44 complexes to obtain one-bond H–Y spin–spin coupling constants (${}^1J_{\text{H-Y}}$) across X–H–Y hydrogen bonds, with Y as the second-period elements ${}^{15}\text{N}$, ${}^{17}\text{O}$, and ${}^{19}\text{F}$. For complexes with traditional hydrogen bonds, the reduced Fermi-contact terms and the reduced one-bond spin–spin coupling constants (${}^1K_{\text{H-Y}}$) are negative. Since ${}^1K_{\text{X-H}}$ has been shown previously to be positive, a change of sign of these two coupling constants must occur along the proton-transfer coordinate. For complexes with symmetric X–H–X hydrogen bonds, the two reduced X–H coupling constants are equal and positive at equilibrium. For complexes stabilized by hydrogen bonds that have some proton-shared character, both ${}^1K_{\text{H-Y}}$ and ${}^1K_{\text{X-H}}$ are also positive. The signs of all three reduced coupling constants (${}^1K_{\text{H-Y}}$, ${}^2K_{\text{X-Y}}$, and ${}^1K_{\text{X-H}}$) that can arise between pairs of hydrogen-bonded atoms are interpreted in terms of the nuclear magnetic resonance triplet wave function model (NMRTWM). Determination of the signs of ${}^1K_{\text{H-Y}}$ and ${}^1K_{\text{X-H}}$ could be useful for confirming the presence or absence of a proton-shared hydrogen bond.

Introduction

There are three spin–spin couplings that can arise between pairs of atoms which form an X–H–Y hydrogen bond. Two are one-bond couplings, the first being coupling between the covalently bonded X and H atoms (${}^1J_{\text{X-H}}$), and the second between the atoms H and Y which form the hydrogen bond (${}^1J_{\text{H-Y}}$). The third coupling is a two-bond coupling between the hydrogen-bonded X and Y atoms (${}^2J_{\text{X-Y}}$). In a series of papers^{1–8} we have presented the results of systematic investigations of two-bond spin–spin coupling constants (${}^2J_{\text{X-Y}}$) across X–H–Y hydrogen bonds, focusing primarily on hydrogen bonds formed from the second period elements ${}^{13}\text{C}$, ${}^{15}\text{N}$, ${}^{17}\text{O}$, and ${}^{19}\text{F}$. In a recent paper, we reexamined the two-bond coupling constants that had been calculated and demonstrated that, except for F–F coupling in the HF dimer,⁸ all reduced Fermi-contact terms and reduced spin–spin coupling constants (${}^2K_{\text{X-Y}}$) are positive.⁹ This is an important result because of its generality and because it allows for the prediction of the signs of the experimentally measured spin–spin coupling constants ${}^2J_{\text{X-Y}}$ across C–H–N, N–H–N, O–H–N, F–H–N, C–H–O, O–H–O, F–H–O, and C–H–F hydrogen bonds. We then turned our attention to the one-bond coupling constants (${}^1J_{\text{X-H}}$) for a set of complexes with ${}^{13}\text{C}$ – ${}^1\text{H}$, ${}^{15}\text{N}$ – ${}^1\text{H}$, ${}^{17}\text{O}$ – ${}^1\text{H}$, and ${}^{19}\text{F}$ – ${}^1\text{H}$ as proton donors and observed that all reduced Fermi-contact terms and reduced spin–spin coupling constants (${}^1K_{\text{X-H}}$) are also positive, in agreement with experimental data for the proton-donor monomers.¹⁰ Insight into the signs of these one- and two-bond coupling constants was gained through the newly formulated nuclear magnetic resonance triplet wave function model (NMRTWM).¹¹ What is needed to complete this investigation of the signs of coupling constants between hydrogen-bonded atoms is an analysis of the remaining one-bond spin–spin coupling constants ${}^1J_{\text{H-Y}}$. It is the purpose of this paper

to present such an analysis for complexes with X–H–Y hydrogen bonds, with Y as the second-period elements ${}^{15}\text{N}$, ${}^{17}\text{O}$, and ${}^{19}\text{F}$.

Method of Calculation

The structures of the hydrogen-bonded complexes investigated in this study have been fully optimized at second-order Møller–Plesset perturbation theory (MP2)^{12–15} with the 6-31+G(d,p) basis set.^{16–19} Harmonic vibrational frequencies were computed to ensure that all structures are equilibrium structures on their potential surfaces.

Spin–spin coupling constants were computed using the equation-of-motion coupled cluster method (EOM-CCSD) in the CI-like approximation,^{20–23} with the Ahlrichs²⁴ qzp basis set on N, O, and F, qz2p on the hydrogen-bonded H atom, and Dunning's cc-pVDZ basis^{25,26} on all other H atoms. In the nonrelativistic approximation, the total spin–spin coupling constant is the sum of four components: the paramagnetic spin–orbit (PSO), diamagnetic spin–orbit (DSO), Fermi-contact (FC), and spin-dipole (SD) terms. All terms were evaluated for most complexes. However, full calculations are not feasible for a few of the complexes included in this study, so only the FC term was evaluated. Approximating ${}^1J_{\text{H-Y}}$ by the FC term was done only when justified by the results of full calculations on similar complexes.

To analyze the effect of changing hydrogen bond type on H–Y coupling constants, structures of N_2H_7^+ ($\text{H}_3\text{N}_a\text{–H}^+ \text{–N}_b\text{H}_3$) were optimized at fixed $\text{N}_a\text{–H}$ distances, starting at $\text{N}_a\text{–H} = 1.00 \text{ \AA}$ and incrementing $\text{N}_a\text{–H}$ in steps of 0.05 to 1.25 \AA . Spin–spin coupling constants were computed for the optimized complex at each $\text{N}_a\text{–H}$ distance. Data for the equilibrium structure of N_2H_7^+ (C_{3v}) which has an $\text{N}_a\text{–H}$ distance of 1.113 \AA , and for the D_{3d} structure which has an $\text{N}_a\text{–H}$ distance of 1.299 \AA , were also included. Similar calculations were performed on the $\text{H}_2\text{OH}^+:\text{NCH}$ complex that has an equilibrium structure with a proton-shared hydrogen bond. Geometry

* To whom correspondence should be addressed.

† Youngstown State University.

‡ Instituto de Química Médica, CSIC.

TABLE 1: Computed X–Y and Y–H Distances (Å) and One-Bond Coupling Constants ($^1J_{\text{H–Y}}$) and Its Components (Hz), and Reduced Coupling Constants [$^1K_{\text{H–Y}}$ ($\text{N A}^{-2} \text{m}^{-3}$) $\times 10^{19}$] for X–H–Y Hydrogen Bonds, with X = ^{15}N , ^{17}O , and ^{19}F

X–H···N		R(X–N)	R(H–N)	PSO	DSO	FC	SD	$^1J_{\text{H–N}}$	$^1K_{\text{H–N}}$
				NCH					
1	NCH:NCH	3.316	2.244	0.2	–0.3	2.1	–0.2	1.8	–1.5
2	F ₃ CH:NCH	3.456	2.373			1.3		1.3 ^a	–1.1
3	HNCH ⁺ :NCH	2.832	1.704	0.5	–0.4	3.2	–0.4	3.5	–2.9
4	CNH:NCH	2.996	1.984	0.3	–0.4	3.3	–0.3	2.9	–2.4
5	pyrrole:NCH	3.160	2.149			2.5		2.5 ^a	–2.1
6	pyridinium:NCH	2.872	1.836			5.1		5.1 ^a	–4.2
7	pyrazinium:NCH	2.833	1.792			5.0		5.0 ^a	–4.1
8	H ₃ NH ⁺ :NCH	2.830	1.781	0.5	–0.4	4.9	–0.4	4.6	–3.8
9	HOH:NCH	3.126	2.159	0.3	–0.4	2.7	–0.2	2.4	–2.0
10	FH:NCH	2.817	1.879	0.4	–0.5	4.2	–0.4	3.7	–3.0
				Azines					
11	NCH:pyridine	3.163	2.080			3.4		3.4 ^a	–2.8
12	CNH:pyridine	2.793	1.753			2.8		2.8 ^a	–2.3
13	FH:pyridine	2.611	1.644			2.1		2.1 ^a	–1.7
14	FH:pyrazine	2.638	1.678			2.9		2.9 ^a	–2.4
				NH ₃					
15	NCH:NH ₃	3.204	2.123	0.3	–0.2	2.8	–0.2	2.7	–2.2
16	F ₃ CH:NH ₃	3.341	2.255			1.9		1.9 ^a	–1.6
17	CNH:NH ₃	2.846	1.811			3.1		3.1 ^a	–2.5
18	pyrrole:NH ₃	3.036	2.015			3.1		3.1 ^a	–2.5
19	FH:NH ₃	2.637	1.673	0.5	–0.5	2.9	–0.3	2.6	–2.1
X–H···O		R(X–O)	R(H–O)	PSO	DSO	FC	SD	$^1J_{\text{H–O}}$	$^1K_{\text{H–O}}$
				CO					
20	NCH:OC	3.478	2.411	0.3	–0.3	0.7	–0.2	0.5	–0.3
21	OCH ⁺ :OC	2.921	1.812	0.7	–0.5	6.0	–0.3	5.9	–3.6
22	HNCH ⁺ :OC	3.079	1.993	0.5	–0.4	4.1	–0.3	3.9	–2.4
23	HCNH ⁺ :OC	2.785	1.752	0.8	–0.6	4.5	–0.4	4.3	–2.6
24	H ₃ NH ⁺ :OC	3.035	2.008	0.5	–0.5	3.8	–0.3	3.5	–2.1
25	FH:OC	3.051	2.124	0.5	–0.6	2.5	–0.3	2.1	–1.3
				H ₂ CO					
26	FH:OCH ₂	2.670	1.743	0.9	–0.7	5.6	–0.8	5.0	–3.1
				H ₂ O					
27	HOH:OH ₂	2.914	1.946	0.6	–0.5	4.9	–0.3	4.7	–2.9
28	FH:OH ₂	2.661	1.718	0.9	–0.6	7.3	–0.4	7.2	–4.4
X–H···F		R(X–F)	R(H–F)	PSO	DSO	FC	SD	$^1J_{\text{H–F}}$	$^1K_{\text{H–F}}$
				HF					
29	NCH:FH	3.216	2.148	–2.2	2.0	–9.9	0.1	–10.0	–0.9
30	OCH ⁺ :FH	2.713	1.601	–4.9	2.9	–68.0	–0.8	–70.8	–6.3
31	HNCH ⁺ :FH	2.862	1.778	–2.5	2.7	–47.0	–0.8	–47.6	–4.2
32	HCNH ⁺ :FH	2.603	1.561	–5.6	3.7	–50.3	–0.1	–52.3	–4.6
33	H ₃ NH ⁺ :FH	2.813	1.808	–1.8	3.2	–42.3	–0.7	–41.6	–3.7
34	H ₂ OH ⁺ :FH	2.523	1.514	–5.5	4.3	–55.1	0.7	–55.6	–4.9
35	FH:FH	2.777	1.856	–4.1	3.9	–28.7	2.0	–26.9	–2.4

^a Estimated from the Fermi-contact term.

optimizations were carried out using the Gaussian 98 suite of programs,²⁷ and coupling constants were obtained using ACES II.²⁸ All calculations were performed on the Cray SV1 or the Itanium Cluster at the Ohio Supercomputer Center.

Results and Discussion

Complexes with Traditional Hydrogen Bonds. Table 1 presents X–Y distances, H–Y distances, $^1J_{\text{H–Y}}$ and its components, and $^1K_{\text{H–Y}}$ for complexes with N, O, or F as the proton acceptor atom. This table is organized so that complexes with X–H–N hydrogen bonds appear first, followed by those with X–H···O and then X–H···F hydrogen bonds. Within each group, the complexes are listed according to the hybridization of the proton-acceptor atom in the order sp, sp², and sp³. For each proton acceptor molecule, complexes with C–H donors are listed first and then N–H, O–H, and F–H. For a given X–H donor, neutral molecules are listed first, followed by cationic proton donors. Within each subgroup, donors are listed according to the hybridization of X in the order sp, sp², and sp³.

The 19 complexes with traditional N–H···N hydrogen bonds comprise by far the most extensive set. The proton acceptors include nitrogen atoms that are sp (HCN), sp² (pyridine and pyrazine), and sp³ (NH₃) hybridized. All complexes have linear N–H···N hydrogen bonds except for HOH:NCH, which has a slightly nonlinear hydrogen bond. For these complexes, the FC term approximates the total H···N coupling constant ($^1J_{\text{H–N}}$) quite well, with the largest difference being 0.5 Hz for FH:NCH. However, the values of $^1J_{\text{H–N}}$ are relatively small, varying between 1 and 5 Hz. These small coupling constants are not surprising in view of the long H–N distances. However, the most interesting feature of these coupling constants is that all $^1J_{\text{H–N}}$ values are positive. Since the magnetogyric ratio of ^1H is positive and that of ^{15}N is negative, all reduced H–N coupling constants ($^1K_{\text{H–N}}$) across X–H–N hydrogen bonds are negative, as seen in Table 1.

The proton acceptors in complexes with X–H···O hydrogen bonds are CO, H₂CO, and H₂O, which have O atoms that are sp, sp², and sp³ hybridized, respectively. The 6 complexes with CO as the proton acceptor have linear X–H···O hydrogen bonds. Since complexes with H₂CO can have hydrogen bonds

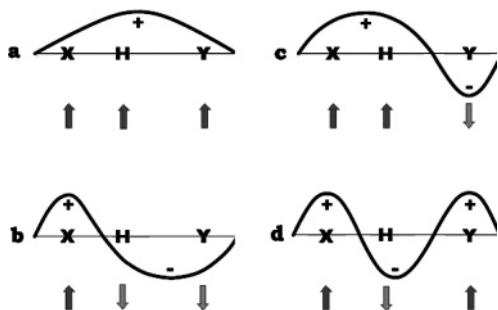


Figure 1. Nodal patterns and nuclear magnetic moment alignments for lower-energy triplet states for a traditional X–H–Y hydrogen bond.

that deviate significantly from linearity because of secondary interactions, only one complex with H_2CO has been included in this study. This complex, $\text{FH}:\text{OCH}_2$, has a hydrogen bond that deviates from linearity by 9° . Two complexes with H_2O as the proton acceptor have been included, and these have slightly nonlinear hydrogen bonds. The H–O coupling constants in complexes with X–H \cdots O hydrogen bonds are again small, ranging from about 0.5 to 7 Hz. The FC term approximates ${}^1J_{\text{H-O}}$ well, with the largest difference of 0.6 Hz found for $\text{FH}:\text{OCH}_2$ which has ${}^1J_{\text{H-O}}$ equal to 5.0 Hz. Once again, all one-bond H–O coupling constants are positive. Since ${}^{17}\text{O}$ has a negative magnetogyric ratio, ${}^1K_{\text{H-O}}$ values are again negative, as seen in Table 1.

Complexes stabilized by X–H \cdots F hydrogen bonds have FH as the proton acceptor molecule. The 7 complexes in this group have hydrogen bonds that deviate slightly from linearity. Table 1 reports the H \cdots F coupling constants for these complexes, which vary from -10 to -71 Hz. Once again, the FC term approximates ${}^1J_{\text{H-F}}$ quite well, with the largest difference found for $\text{OCH}^+:\text{FH}$, in which case the FC term and ${}^1J_{\text{H-F}}$ are -68.0 and -70.8 Hz, respectively. Since ${}^1\text{H}$ and ${}^{19}\text{F}$ have positive magnetogyric ratios, ${}^1J_{\text{H-F}}$ and ${}^1K_{\text{H-F}}$ are negative.

As is well-known, reduced coupling constants, K_{AB} , are used when comparing coupling between difference pairs of elements in order to remove the dependence on the magnetogyric ratios of the coupled atoms A and B. It is significant that the values of ${}^1K_{\text{H-Y}}$ are negative for all H \cdots Y coupling constants reported in Table 1 for complexes with traditional X–H \cdots N, X–H \cdots O, and X–H \cdots F hydrogen bonds, independent of the nature of the proton donor X–H. Thus, with the single exception of F–F coupling between two HF molecules, ${}^1K_{\text{X-H}}$ and ${}^2K_{\text{X-Y}}$ are positive, whereas ${}^1K_{\text{H-Y}}$ is negative for hydrogen-bonded complexes involving second-period elements. Since the Fermi-contact term is the dominant term for determining J , insight into the positive signs of the reduced Fermi-contact terms for

one-bond X–H and two-bond X–Y coupling (and therefore ${}^1K_{\text{X-H}}$ and ${}^2K_{\text{X-Y}}$) was previously gained from the nuclear magnetic resonance triplet wave function model (NMRTWM).¹¹ This model relates the sign of the contribution to the reduced FC term from a given sigma-type triplet state in the sum-over-states expression for the FC term²⁹ to the nodal patterns of the excited-state wave function and the orientation of the coupled magnetic nuclei.

Figure 1 shows the nodal patterns for low-energy triplet-state wave functions that have zero, one, or two nodes intersecting the X–Y axis. In terms of these states, those that dominate ${}^1K_{\text{X-H}}$ could have either one node intersecting the X–Y axis through the X–H covalent bond (Figure 1b) or two nodes, one intersecting the X–H covalent bond and the other the H \cdots Y hydrogen bond (Figure 1d). In both types of states, the orientation of the nuclear magnetic moments of X and H are antiparallel. For ${}^2K_{\text{X-Y}}$, states with one node intersecting the X–Y axis either between the X–H covalent bond (Figure 1b) or the H \cdots Y hydrogen bond (Figure 1c) make positive contributions and must therefore dominate. The data obtained in the present study show that the signs of ${}^1K_{\text{H-Y}}$ are negative, suggesting that states with either no nodes (Figure 1a) or one node intersecting the X–H covalent bond (Figure 1b) must dominate, although the number of excited triplet states with no nodes is expected to be small. What is of utmost significance is the observation that the signs of ${}^1K_{\text{X-H}}$, ${}^2K_{\text{X-Y}}$, and ${}^1K_{\text{H-Y}}$ are consistent with the dominant role of triplet states with wave functions that have one node (Figure 1b) (or an odd number of nodes) intersecting the covalent X–H bond, and no nodes (or an even number of nodes) intersecting the H \cdots Y hydrogen bond. Thus, these data suggest that triplet states with the same nodal patterns are dominant for the three coupling constants which arise between the atoms that form the X–H–Y hydrogen bond. The magnitude of the contribution to ${}^1K_{\text{X-H}}$, ${}^2K_{\text{X-Y}}$, and ${}^1K_{\text{H-Y}}$ from each state cannot be determined without a full sum-over-states calculation, which is not feasible.^{29,30}

Since ${}^1K_{\text{X-H}}$ and ${}^2K_{\text{X-Y}}$ are positive and ${}^1K_{\text{H-Y}}$ is negative for complexes with traditional hydrogen bonds, it is possible to predict the signs of experimentally measured one- and two-bond coupling constants across X–H \cdots Y hydrogen bonds. The predicted signs are given in Table 2. Since the magnetogyric ratio of ${}^1\text{H}$ is positive, ${}^1J_{\text{X-H}}$ is positive if the magnetogyric ratio of X is positive, and ${}^1J_{\text{H-Y}}$ is positive if the magnetogyric ratio of Y is negative. ${}^2J_{\text{X-Y}}$ is positive if neither or both X or Y have negative magnetogyric ratios.

Complexes with Proton-Shared Hydrogen Bonds. Since ${}^1K_{\text{X-H}}$ is positive and ${}^1K_{\text{H-Y}}$ is negative for complexes with traditional hydrogen bonds, there must be a change in the signs

TABLE 2: Summary of the Predicted Signs of One- and Two-Bond Spin–Spin Coupling Constants across X–H–Y Hydrogen Bonds

	Traditional Hydrogen Bonds
sign of ${}^1K_{\text{X-H}}$ +	sign of ${}^1J_{\text{X-H}}$ + for X = ${}^{13}\text{C}$ and ${}^{19}\text{F}$ – for X = ${}^{15}\text{N}$ and ${}^{17}\text{O}$
sign of ${}^1K_{\text{H-Y}}$ –	sign of ${}^1J_{\text{H-Y}}$ – for Y = ${}^{13}\text{C}$ and ${}^{19}\text{F}$ + for Y = ${}^{15}\text{N}$ and ${}^{17}\text{O}$
sign of ${}^2K_{\text{X-Y}}$ +	sign of ${}^2J_{\text{X-Y}}$ + if the magnetogyric ratios of neither or both X and Y are negative – if the magnetogyric ratio of either X or Y is negative
signs of ${}^1K_{\text{X-H}}$ and ${}^1K_{\text{H-Y}}$ +	Symmetric or Quasisymmetric Hydrogen Bonds signs of ${}^1J_{\text{X-H}}$ and ${}^1J_{\text{H-Y}}$ + when X = ${}^{13}\text{C}$ and ${}^{19}\text{F}$ – when X = ${}^{15}\text{N}$ and ${}^{17}\text{O}$
sign of ${}^2K_{\text{X-Y}}$ +	sign of ${}^2J_{\text{X-Y}}$ + if the magnetogyric ratios of neither or both X and Y are negative – if the magnetogyric ratio of either X or Y is negative

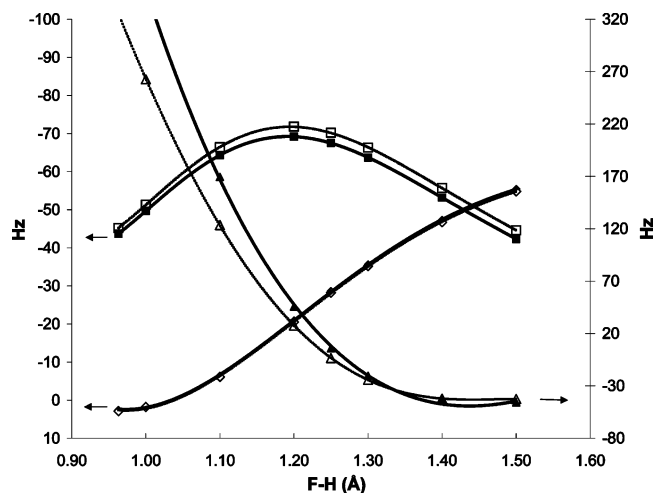


Figure 2. The variation of coupling constants as a function of the F–H distance in FH:NH₃. Fermi-contact terms, open symbols; total J, filled symbols; triangles: F–H coupling; diamonds, H–N coupling; squares, F–N coupling.

of the X–H and H–Y coupling constants as the proton is transferred from X to Y and the ion-pair X[−]⋯⁺H–Y is formed. Sign changes of coupling constants have been observed experimentally by Limbach and co-workers in studies of the temperature dependence of F–H and H–N coupling constants for the FH:collidine complex.^{31–33} These investigators interpreted their experimental results in terms of proton transfer from F to N as a function of temperature and solvent ordering. Our calculations also indicated that F–H and H–N coupling constants change sign as the proton is transferred from F to N in the FH:NH₃ and FH:pyridine complexes, which were used as models for FH:collidine.³⁴ The variation of ¹J_{F–H}, ¹J_{H–N}, and ²J_{F–N} along the proton-transfer coordinate is illustrated for FH:NH₃ in Figure 2.

Perhaps the simplest approach for examining changes in the signs of one-bond coupling constants as a function of proton transfer is to focus on ¹J_{X–H} and ¹J_{H–Y} for a complex that may have a symmetric hydrogen bond, such as N₂H₇⁺. Although the equilibrium structure of N₂H₇⁺ has C_{3v} symmetry with N–H

distances of 1.113 and 1.591 Å, there is a transition structure of D_{3d} symmetry that has a symmetric N_a⋯H⋯N_b hydrogen bond. In this structure, the N–H distances are 1.299 Å, and the two N–H distances (J_{N_a–H}) and (J_{H–N_b}) have equal values of −26.5 Hz. How these coupling constants change as the proton is transferred from one nitrogen (N_a) to the other (N_b) is illustrated in Figure 3. At an N_a–H distance of 1.00 Å, J_{N_a–H} is −73.2 Hz and J_{H–N_b} is +3.3 Hz. As the proton moves from N_a to N_b, ¹J_{H–N_b} must pass through 0.0 Hz and then become negative and equal to J_{N_a–H} when the hydrogen bond is symmetric. As the proton continues to move toward N_b, the N_b–H coupling constant becomes more negative and the N_a–H coupling constant eventually becomes positive as N_b–H becomes the proton donor and N_a the proton acceptor. It is interesting that ¹J_{H–N_b} changes sign near the equilibrium N_a–H distance of 1.113 Å. This explains the very small value of −0.3 Hz for ¹J_{H–N_b} for the equilibrium C_{3v} structure of N₂H₇⁺.

The equilibrium structures of (HCN)₂H⁺, (H₂O)₂H⁺, (CO)₂H⁺, and (HF)₂H⁺ have symmetric hydrogen bonds, and ¹K_{X–H} and ¹K_{H–X} are equal and positive for each complex. Can these signs be explained by NMRTWM? For ease of discussion, we focus only on those triplet states with wave functions that have zero, one, or two nodes intersecting the hydrogen bonding axis between the two X atoms, as illustrated in Figure 4. As noted above in the discussion of the signs of reduced one- and two-bond coupling constants for traditional hydrogen bonds, the dominance of states with one node intersecting the hydrogen-bonding axis through the X–H covalent bond is consistent with the signs of ¹K_{X–H}, and ¹K_{H–Y}. What happens to the contributions from such states when the hydrogen bond is a symmetric proton-shared X⋯H⋯X hydrogen bond? For symmetric hydrogen bonds, wave functions with a single node must have that node intersecting the hydrogen-bonding axis through the hydrogen-bonded proton, as illustrated in Figure 4b. Contributions to the two X–H coupling constants from states with such wave functions must be zero. Thus, the states that must dominate ¹J_{X–H} and ¹J_{H–X} (and make ¹K_{X–H} and ¹K_{H–X} positive) have wave functions with an odd number of nodes intersecting each X–H bond, as illustrated in Figure 4c. Moreover, similar states are expected to dominate in complexes that have quasi-symmetric hydrogen bonds, such as COH⁺:FH (or HFH⁺: OC)

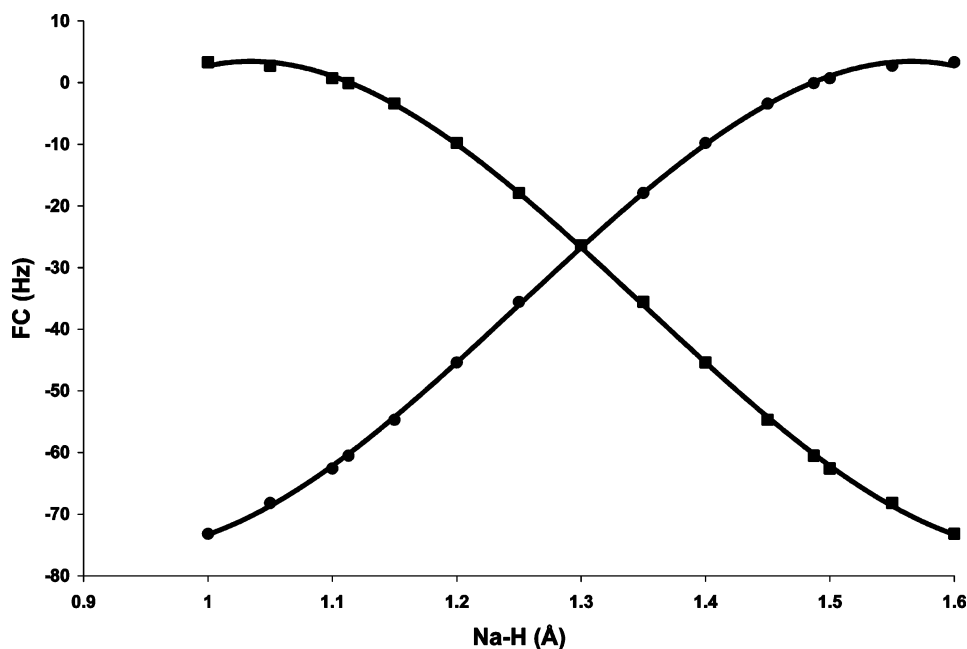


Figure 3. The variation of the Fermi-contact term for N_a–H and H–N_b coupling in N₂H₇⁺ (H₃N_a–H⋯N_bH₃)⁺ as a function of the N_a–H distance. Solid circles, FC term for N_a–H; solid squares, FC term for H–N_b.

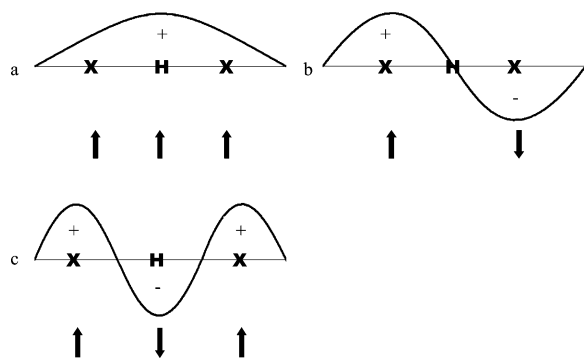


Figure 4. Nodal patterns and nuclear magnetic moment alignments for lower-energy triplet states for a symmetric X...H...X hydrogen bond.

and $\text{H}_2\text{OH}^+:\text{NCH}$ (or $\text{HCNH}^+:\text{OH}_2$). As evident from Table 3, these complexes have positive values of both ${}^1K_{\text{X-H}}$ and ${}^1hK_{\text{H-Y}}$. Somewhere along the proton-transfer coordinate, the sign of one of these coupling constants must change, depending on whether the H atom approaches X or Y. The data of Table 1 show that ${}^1hJ_{\text{H-Y}}$ is small for complexes with traditional X-H...Y hydrogen bonds. Thus, the change of sign of ${}^1hK_{\text{H-Y}}$ must occur at an H-Y distance that corresponds to a X-H distance that is slightly longer than the X-H equilibrium distance in a complex with a traditional X-H...Y hydrogen bond. This can be seen for the $\text{H}_2\text{OH}^+:\text{NCH}$ complex in Figure 5, which shows that ${}^1hJ_{\text{H-N}}$ changes sign at an O-H distance similar to that in H_3O^+ . Figure 2 shows that ${}^1hJ_{\text{H-N}}$ changes

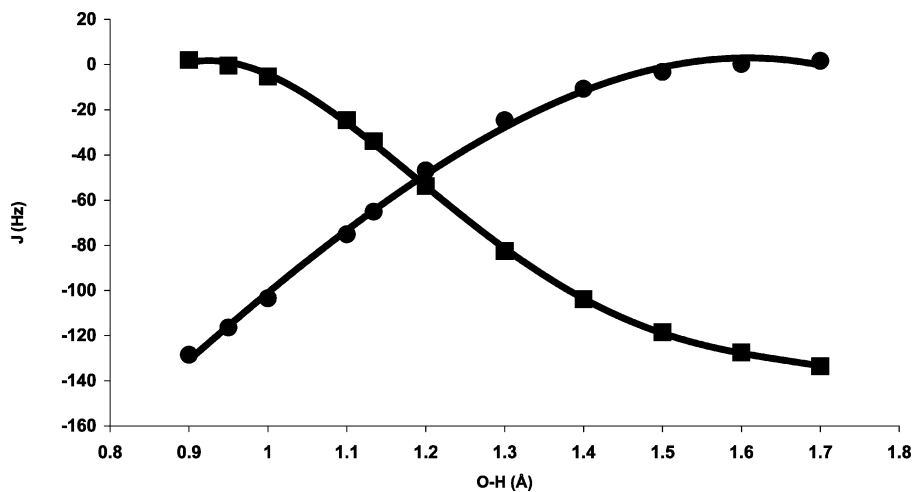


Figure 5. The variation of hydrogen-bonded O-H and H-N coupling constants for $\text{H}_2\text{O}-\text{H}^+\cdots\text{NCH}$ as a function of the O-H distance. Solid circles, $J_{\text{O-H}}$; Solid squares, $J_{\text{H-N}}$.

TABLE 3: Computed X-Y and Y-H Distances (Å) and One-Bond Coupling Constants (${}^1hJ_{\text{H-Y}}$) and Its Components (Hz), and Reduced Coupling Constants [${}^1hK_{\text{H-Y}}$ ($\text{N A}^{-2} \text{m}^{-3}$) $\times 10^{19}$] for X-H-Y Hydrogen Bonds with Significant Proton-Shared Character

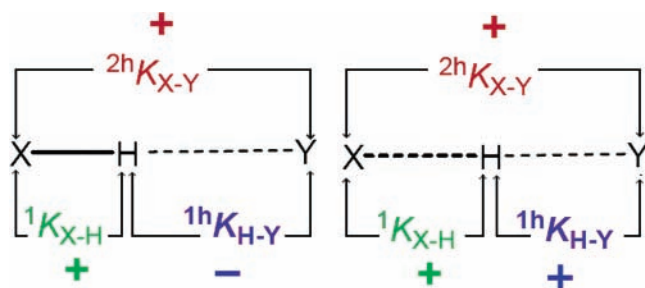
		R(X-Y)	R(Y-H)	PSO	DSO	FC	SD	${}^1hJ_{\text{H-Y}}$	${}^1hK_{\text{H-Y}}$
Symmetric Hydrogen Bonds									
N...H...N									
35	$(\text{HCN})_2\text{H}^+ D_{\infty h}$	2.521	1.260	0.7	-0.4	-56.3	-0.6	-56.6	46.5
36	$(\text{NH}_3)_2\text{H}^+ D_{3d}$	2.598	1.299	0.4	-0.3	-26.4	-0.2	-26.5	21.8
O...H...O									
37	$(\text{H}_2\text{O})_2\text{H}^+ C_2$	2.386	1.193	0.6	-0.6	-47.5	0.0	-47.5	29.2
38	$(\text{CO})_2\text{H}^+ D_{\infty h}$	2.394	1.197	1.0	-0.7	-68.0	-0.5	-68.2	41.9
F...H...F									
39	$(\text{HF})_2\text{H}^+ C_{2h}$	2.302	1.151	8.8	4.0	186.3	-3.8	195.3	17.3
Quasisymmetric Proton-Shared Hydrogen Bonds									
40	$\text{H}_3\text{NH}^+:\text{NH}_3 C_{3v}$	2.704	1.591	0.5	-0.4	-0.1	-0.3	-0.3	-0.2
41	$\text{COH}^+:\text{FH}$	2.362	1.093	18.8	2.9	298.9	-5.3	315.3	27.9
42	$\text{HFH}^+:\text{OC}$	2.362	1.271	1.1	-0.9	-39.3	-0.6	-39.7	24.4
43	$\text{H}_2\text{OH}^+:\text{NCH}$	2.471	1.337	0.7	-0.5	-33.9	-0.6	-34.3	28.2
44	$\text{HCNH}^+:\text{OH}_2$	2.471	1.134	0.0	-0.4	-65.1	0.1	-65.4	40.1

sign at an F-H distance slightly longer than the equilibrium F-H distance in the $\text{FH}:\text{NH}_3$ complex.

For all types of hydrogen bonds, lower-energy triplet states that have wave functions with one node intersecting the X-H bond dominate and make ${}^2hK_{\text{X-Y}}$ and ${}^1K_{\text{X-H}}$ positive. These same states also dominate and make ${}^1hK_{\text{H-Y}}$ negative when the hydrogen bond is traditional. However, when the hydrogen bond is symmetric, the dominate states for ${}^1K_{\text{X-H}}$ and ${}^1hK_{\text{H-Y}}$ are those with one node (or an odd number of nodes) intersecting the X-H bond and one node (or an odd number of nodes) intersecting the H...Y hydrogen bond, as illustrated in Figure 4c. There must be a smooth transition in the states that dominate the reduced spin-spin coupling constants as the hydrogen-bonded proton moves along the proton-transfer coordinate. The signs of ${}^2hK_{\text{X-Y}}$, ${}^1K_{\text{X-H}}$, and ${}^1hK_{\text{H-Y}}$ for traditional and proton-shared hydrogen bonds are summarized in Scheme 1.

The results of this study suggest that the signs of the two one-bond spin-spin coupling constants could be used to detect the presence of a proton-shared (or low-barrier) hydrogen bond. If the signs of ${}^1hK_{\text{H-Y}}$ and ${}^1K_{\text{X-H}}$ are the same, then the hydrogen bond is proton-shared or has moved far enough along the proton-transfer coordinate to acquire proton-shared character. This prediction is in agreement with the signs of the two one-bond spin-spin coupling constants reported by Limbach and co-workers for the proton-shared complex of HF with collidine.³¹⁻³³ These investigators reported values of +30 and -50 Hz for ${}^1J_{\text{F-H}}$ and ${}^1hJ_{\text{H-N}}$, respectively, for an $\text{FH}:\text{collidine}$ complex with a proton-shared hydrogen bond. Thus, both ${}^1K_{\text{F-H}}$ and ${}^1hK_{\text{H-N}}$ are positive for this complex.

SCHEME 1



In our recent study of X–H spin–spin coupling constants across X–H–Y hydrogen bonds,¹⁰ we demonstrated that all $^1K_{X-H}$ (and $^1J_{X-H}$) for X = ^{13}C , ^{15}N , ^{17}O , and ^{19}F could be linearly related to the X–H distances times the square of the Pauling electronegativity of X. We were not able to find a similar relationship for $\text{Y}\cdots\text{H}$ coupling constants. In our opinion, the difficulties in doing this arise from the relatively small values of $^1hJ_{H-Y}$, particularly for complexes with traditional hydrogen bonds, and from the sensitivity of both the sign and magnitude of $^1hJ_{H-Y}$ to hydrogen bond type.

Conclusions

The following statements are supported by the computed EOM-CCSD H–Y spin–spin coupling constants ($^1hJ_{H-Y}$) across X–H–Y hydrogen bonds for Y = ^{15}N , ^{17}O , and ^{19}F .

1. For traditional hydrogen bonds, all reduced Fermi-contact terms and reduced spin–spin coupling constants ($^1hK_{H-Y}$) are negative, independent of the nature of the X–H donor.

2. For traditional hydrogen bonds, $^1K_{X-H}$ and $^2hK_{X-Y}$ are positive, and $^1hK_{H-Y}$ is negative. The nuclear magnetic resonance triplet wave function model (NMRTWM) suggests that among lower-energy excited sigma-type triplet states, those with wave functions that have a single node (or an odd number of nodes) intersecting the X–H covalent bond and no nodes (or an even number of nodes) intersecting the $\text{H}\cdots\text{Y}$ hydrogen bond are important in determining the signs of these reduced coupling constants.

3. There must be a change in the signs of $^1K_{X-H}$ and $^1hK_{H-Y}$ along the proton-transfer coordinate.

a. For symmetric hydrogen bonds, $^1K_{X-H}$ and $^1hK_{H-X}$ are equal and positive at equilibrium. Since wavefunctions for triplet states with an odd number of nodes must have one node passing through the H atom, dominate lower-energy states must have one node (or an odd number of nodes) intersecting each X–H bond.

b. For complexes stabilized by hydrogen bonds that have acquired some proton-shared character, both $^1K_{X-H}$ and $^1hK_{H-Y}$ are also positive. There must be a smooth change in the values of coupling constants and a smooth transition among those triplet states that determine coupling constants along the proton-transfer coordinate.

4. The generalizations made concerning the signs of one- and two-bond spin–spin coupling constants that can arise between pairs of atoms that form an X–H–Y hydrogen bond enable the prediction of the signs of the experimentally measured coupling constants, taking into account the magnetogyric ratios of the hydrogen-bonded atoms. Since $^1K_{X-H}$ and $^1hK_{H-Y}$ are both positive for hydrogen bonds with some proton-shared character, determination of the signs of these coupling constants may serve as a tool for confirming the presence or absence of a proton-shared hydrogen bond.

Acknowledgment. This work was supported by a grant from the U.S. National Science Foundation (NSF CHE-9873815) and

by the Spanish DGI/MCyT (project No. BQU-2003-01251). The authors gratefully acknowledge this support and that of the Ohio Supercomputer Center.

References and Notes

- (1) Del Bene, J. E.; Jordan, M. J. T.; Perera, S. A.; Bartlett, R. J. *J. Phys. Chem. A* **2001**, *105*, 8399.
- (2) Del Bene, J. E.; Perera, S. A.; Bartlett, R. J. *J. Chem. Phys. A* **2001**, *105*, 930.
- (3) Del Bene, J. E.; Perera, S. A.; Bartlett, R. J. *Magn. Reson. Chem.* **2001**, *39*, S109.
- (4) Toh, J.; Jordan, M. J. T.; Husowitz, B. C.; Del Bene, J. E. *J. Phys. Chem. A* **2001**, *105*, 10906.
- (5) Del Bene, J. E.; Perera, S. A.; Bartlett, R. J.; Yáñez, M.; M6, O.; Elguero, J.; Alkorta, I. *J. Phys. Chem. A* **2003**, *107*, 3121.
- (6) Del Bene, J. E.; Perera, S. A.; Bartlett, R. J.; M6, O.; Yáñez, M.; Elguero, J.; Alkorta, I. *J. Phys. Chem. A* **2003**, *107*, 3126.
- (7) Del Bene, J. E.; Perera, S. A.; Bartlett, R. J.; M6, O.; Yáñez, M.; Elguero, J.; Alkorta, I. *J. Phys. Chem. A* **2003**, *107*, 3222.
- (8) Del Bene, J. E.; Elguero, J.; Alkorta, I.; Yáñez, M.; M6, O. *J. Chem. Phys.* **2004**, *120*, 3237.
- (9) Del Bene, J. E.; Elguero, J. *Magn. Reson. Chem.* **2004**, *42*, 421.
- (10) Del Bene, J. E.; Elguero, J. *J. Am. Chem. Soc.* (in press).
- (11) Del Bene, J. E.; Elguero, J. *J. Chem. Phys. Lett.* **2003**, *382*, 100.
- (12) Pople, J. A.; Binkley, J. S.; Seeger, R. *Int. J. Quantum Chem. Quantum Chem. Symp.* **1976**, *10*, 1.
- (13) Krishnan, R.; Pople, J. A. *Int. J. Quantum Chem.* **1978**, *14*, 91.
- (14) Bartlett, R. J.; Silver, D. M. *J. Chem. Phys.* **1975**, *62*, 3258.
- (15) Bartlett, R. J.; Purvis, G. D. *Int. J. Quantum Chem.* **1978**, *14*, 561.
- (16) Hehre, W. J.; Ditchfield, R.; Pople, J. A. *J. Chem. Phys.* **1982**, *56*, 2257.
- (17) Hariharan, P. C.; Pople, J. A. *Theor. Chim. Acta* **1973**, *238*, 213.
- (18) Spitznagel, G. W.; Clark, T.; Chandrasekhar, J.; Schleyer, P. v. R. *J. Comput. Chem.* **1982**, *3*, 3633.
- (19) Clark, T.; Chandrasekhar, J.; Spitznagel, G. W.; Schleyer, P. v. R. *J. Comput. Chem.* **1983**, *4*, 294.
- (20) Perera, S. A.; Sekino, H.; Bartlett, R. J. *J. Chem. Phys.* **1994**, *101*, 2186.
- (21) Perera, S. A.; Nooijen, M.; Bartlett, R. J. *J. Chem. Phys.* **1996**, *104*, 3290.
- (22) Perera, S. A.; Bartlett, R. J. *J. Am. Chem. Soc.* **1995**, *117*, 8476.
- (23) Perera, S. A.; Bartlett, R. J. *J. Am. Chem. Soc.* **1996**, *118*, 7849.
- (24) Schäfer, A.; Horn, H.; Ahlrichs, R. *J. Chem. Phys.* **1992**, *97*, 2571.
- (25) Dunning, T. H., Jr. *J. Chem. Phys.* **1989**, *90*, 1007.
- (26) Woon, D. E.; Dunning, T. H., Jr. *J. Chem. Phys.* **1995**, *103*, 4572.
- (27) Frisch, M. J.; Trucks, G. W.; Schlegel, H. B.; Scuseria, G. E.; Robb, M. A.; Cheeseman, J. R.; Zakrzewski, V. G.; Montgomery, J. A., Jr.; Stratmann, R. E.; Burant, J. C.; Dapprich, S.; Millam, J. M.; Daniels, A. D.; Kudin, K. N.; Strain, M. C.; Farkas, O.; Tomasi, J.; Barone, V.; Cossi, M.; Cammi, R.; Mennucci, B.; Pomelli, C.; Adamo, C.; Clifford, S.; Ochterski, J.; Petersson, G. A.; Ayala, P. Y.; Cui, Q.; Morokuma, K.; Malick, D. K.; Rabuck, A. D.; Raghavachari, K.; Foresman, J. B.; IOSlowski, J.; Ortiz, J. V.; Stefanov, B. B.; Liu, G.; Liashenko, A.; Piskorz, P.; Komaromi, I.; Gomperts, R.; Martin, R. L.; Fox, D. J.; Keith, T.; Al-Laham, M. A.; Peng, C. Y.; Nanayakkara, A.; Gonzalez, C.; Challacombe, M.; Gill, P. M. W.; Johnson, B. G.; Chen, W.; Wong, M. W.; Andres, J. L.; Head-Gordon, M.; Replogle, E. S.; Pople, J. A. Gaussian 98, revision A.9; Gaussian, Inc.: Pittsburgh, PA, 1998.
- (28) ACES II is a program product of the Quantum Theory Project, University of Florida. Authors: Stanton, J. F.; Gauss, J.; Watts, J. D.; Nooijen, M.; Oliphant, N.; Perera, S. A.; Szalay, P. G.; Lauderdale, W. J.; Gwaltney, S. R.; Beck, S.; Balkov, A.; Bernholdt, D. E.; Baeck, K.-K.; Tozyczko, P.; Sekino, H.; Huber, C.; Bartlett, R. J. Integral packages included are VMOL (Almlöf J, Taylor PR); VPROPS (Taylor PR); ABACUS (Helgaker, T., Jensen, H. J. Aa, Jorgensen, P., Olsen, J., Taylor, P. R.). Brillouin-Wigner perturbation theory was implemented by Pittner, J.
- (29) Kirpekar, S.; Jensen, H. J. Aa; Oddershede, J. *J. Chem. Phys.* **1994**, *188*, 171.
- (30) Sekino, H.; Bartlett, R. J. In *Nonlinear Optical Materials*; Karna, S., Ed.; American Chemical Society: Washington, DC, 1994.
- (31) Shenderovich, I. G.; Burtsev, A. P.; Denisov, G. S.; Golubev, N. S.; Limbach, H.-H. *Magn. Reson. Chem.* **2001**, *39*, S91.
- (32) Golubev, N. S.; Shenderovich, I. G.; Smirnov, S. N.; Denisov, G. S.; Limbach, H.-H. *J. Chem. Eur. J.* **1999**, *5*, 492.
- (33) Shenderovich, I. G.; Tolstoy, P. M.; Golubev, N. S.; Smirnov, S. N.; Denisov, G. S.; Limbach, H.-H. *J. Am. Chem. Soc.* **2003**, *125*, 11710.
- (34) Del Bene, J. E.; Bartlett, R. J.; Elguero, J. *Magn. Reson. Chem.* **2002**, *40*, 767.